



**HAL**  
open science

## New results on the model problem of the diffusion of turbulence from a plane source.

Jean-Bernard Cazalbou, Patrick Chassaing

► **To cite this version:**

Jean-Bernard Cazalbou, Patrick Chassaing. New results on the model problem of the diffusion of turbulence from a plane source.. *Physics of Fluids*, 2001, 1 (2), pp.0. 10.1063/1.1336155 . hal-03609996

**HAL Id: hal-03609996**

**<https://hal.science/hal-03609996>**

Submitted on 16 Mar 2022

**HAL** is a multi-disciplinary open access archive for the deposit and dissemination of scientific research documents, whether they are published or not. The documents may come from teaching and research institutions in France or abroad, or from public or private research centers.

L'archive ouverte pluridisciplinaire **HAL**, est destinée au dépôt et à la diffusion de documents scientifiques de niveau recherche, publiés ou non, émanant des établissements d'enseignement et de recherche français ou étrangers, des laboratoires publics ou privés.

## New results on the model problem of the diffusion of turbulence from a plane source

J.-B. Cazalbou<sup>a)</sup> and P. Chassaing

*ENSICA, 1 place Émile Blouin, 31056 Toulouse cedex 5, France*

(Received 23 December 1999; accepted 6 November 2000)

The problem of the diffusion of turbulence from a plane source is addressed in the context of two-equation eddy-viscosity models and Reynolds-stress-transport models. In the steady state, full analytic solutions are given. At second order, they provide the equilibrium value of the anisotropy level obtained with different combinations of return-to-isotropy and turbulent-diffusion schemes and confirm the results obtained by Straatman *et al.* [AIAA J. **36**, 929 (1998)] in an approximate analysis. In addition, all the characteristics of the turbulence decrease can be determined and it is shown that a special constraint on the value of the modeling constants should hold if turbulence fills the whole surrounding space. In a second step, precise results can be given for the unsteady model problem at the first-order-closure level. The evolution cannot be described with a single set of characteristic scales and one has to distinguish the cases of short and large times. In the short-time regime, the flow is governed by the characteristic scales of turbulence at the source and contamination of the flow proceeds as  $t^{1/2}$ . At large times, the flow is governed by time-dependent characteristic scales that correspond to the solution of the steady problem at the instantaneous location of the front. Contamination of the flow proceeds as a power of time that can be related to the value of the modeling constants. The role of a combination of these constants is emphasized whose value can be specified to produce a solution that matches simultaneously the experimental data for the decrease of turbulent kinetic energy in the steady state and the exponent of the propagation velocity in the transient regime. © 2001 American Institute of Physics.

[DOI: 10.1063/1.1336155]

### I. INTRODUCTION

We consider the action of a plane source of turbulence on a fluid initially at rest in an unbounded domain. Turbulence is supposed to be statistically homogeneous in the plane of the source with known characteristic scales. Theoretical arguments by Corrsin and Kistler<sup>1</sup> show that, as the source is switched on, turbulence proceeds in the undisturbed fluid behind a perfectly defined although highly irregular interface. After a sufficient time, all the surrounding space is filled with turbulence and a steady state of spatial decay is reached in which the local level of turbulent kinetic energy results from a balance between turbulent diffusion from the source and local destruction by viscous dissipation. Turbulent diffusion is therefore an essential mechanism in this situation which distinguishes it from classical situations of temporal or spatial decay of homogeneous turbulence.

In practice, this situation can be obtained with a turbulence grid oscillating perpendicularly to its plane in the absence of mean velocity. Long<sup>2</sup> studied theoretically such a situation. By a discussion of relevant parameters, dimensional analysis and a simple model for the grid-generated motions, he obtained some remarkable results: in the steady state, the turbulent length scale increases linearly with the distance from the source ( $z$ ), the rms value of the velocity

fluctuation is proportional to  $z^{-1}$ ; during the propagation, the mean position of the interface proceeds as  $t^{1/2}$ , where  $t$  is the time counted from a conveniently chosen origin. These results allow a concept of “grid action” to be introduced, according to which the flow is governed by a single parameter: the “action” parameter<sup>3</sup>  $K \propto u' l$ , where  $u'$  and  $l$  are, respectively, the rms value of the velocity fluctuation along  $x$  (perpendicular to  $z$ ) and the turbulent length scale at the same location in  $z$ .  $K$  has the dimension of viscosity and, according to Long’s analysis, is constant throughout the flow.

A significant number of experimental studies helps to evaluate Long’s conclusions. A linear variation for the length scale is of little doubt being confirmed by Thompson and Turner,<sup>4</sup> Hopfinger and Toly,<sup>5</sup> Kit, Strang and Fernando<sup>6</sup> and by the direct-numerical-simulation results of Briggs *et al.*<sup>7</sup> Such an agreement is not observed for the decay of turbulence. If most of the data exhibits the  $z^{-1}$  behavior for the decay of  $u'$  (Hopfinger and Toly,<sup>5</sup> Hannoun, Fernando and List,<sup>8</sup> De Silva and Fernando,<sup>9,10</sup> Kit *et al.*<sup>6</sup>), some authors give significantly different values for the decay exponent:  $-1.5$  for Thompson and Turner,<sup>4</sup> varying between  $-0.86$  and  $-1.5$  for Nokes<sup>11</sup> and  $-1.35$  in the simulation by Briggs *et al.*<sup>7</sup> It should be noted, however, that Thompson and Turner’s data have been reinterpreted by Hopfinger and Toly and that some of them seem to support the  $z^{-1}$  behavior, while a low-Reynolds-number effect could be present in the simulation results of Briggs *et al.* Experiment also gives informa-

<sup>a)</sup>Author to whom correspondence should be addressed. Telephone: (33) 5 61 61 86 59; Fax: (33) 5 61 61 86 63; Electronic mail: cazalbou@ensica.fr

tion on the anisotropy of turbulence: diffusion only acts along  $z$  and velocity fluctuations are enhanced in this direction. The data<sup>5,6,8-10</sup> for the ratio of the rms fluctuations along  $z$  and  $x$  ( $a=w'/u'$ ) are scattered in the range 1.1 to 1.32 while the simulation gives a value of 1.4.

Now, if we turn to the case of the propagation regime, the experiments of Dickinson and Long<sup>3,12</sup> deal with homogeneous fluids and support the  $t^{1/2}$  behavior for the mean position of the interface. Other studies by Fernando<sup>13</sup> and De Silva and Fernando<sup>9</sup> deal with stratified fluids, the data also confirm the  $t^{1/2}$  behavior at the beginning of the evolution when gravity effects are negligible.

The model problem associated with the steady state has been studied for the  $(k, \epsilon)$  turbulence model of Jones and Launder<sup>14</sup> by Sonin<sup>15</sup> and for the  $(k, \epsilon)$ ,  $(k, kL)$ <sup>16</sup> and  $(k, \omega)$ <sup>17</sup> models by Briggs *et al.*<sup>7</sup> In all cases, solutions in powers of  $z$  for the turbulent quantities and a linear variation of the length scale are obtained. At the second-order-closure level, Straatman, Stubbley and Raithby<sup>18</sup> examined the anisotropy level far from the source with different combinations of turbulent-diffusion and return-to-isotropy schemes. The analysis is based on the hypothesis that the velocity fluctuations and the dissipation rate evolve, respectively, as  $z^{-1}$  and  $z^{-4}$  (consistently with a linear variation of the length scale). The value of the anisotropy ratio  $a$  can be obtained and the authors show that an adequate modeling of pressure diffusion is essential to a good prediction of the anisotropy. A slight modification to Lumley's model<sup>19</sup> is proposed, which brings the results in good agreement with known data.

In the case of the propagation regime, information on the solution have been given by Spalart and Allmaras<sup>20</sup> for their one-equation model and by Cazalbou, Spalart and Bradshaw<sup>21</sup> for a variety of two-equation models. Both studies show that, with some special restriction on the values of the modeling constants, a weak solution (discontinuous for some of the derivatives at a finite distance from the source) to the model problem is obtained. This property—linked with the nonlinearity of the diffusion model—corresponds *as in reality* to a turbulent front that propagates into the undisturbed fluid at a finite velocity. In the vicinity of the front, the form of the solution can be given as a function of local characteristic scales. Unfortunately, these cannot be related to global scales in the absence of a complete solution of the problem.

The present paper is divided into two parts. In the first part we revisit the model problem for the steady state. We show that power solutions are the only self-similar solutions and that the hypothesis made in Straatman *et al.* are unnecessary. Exact and complete solutions are therefore available for first- and second-order turbulence models. The second part is restricted to the case of first-order-closure models for which we show that the knowledge of the steady solution allows to precise the meaning and behavior of the characteristic scales that govern the propagation. The time evolution of the position of the front can then be characterized directly as a function of the modeling constants.

## II. STEADY PROBLEM

We consider a plane source of turbulence whose characteristics are constant in the  $(x, y)$  plane. Turbulence diffuses along  $z$  in the surrounding space initially at rest and we are interested in the steady state obtained in the half space  $z > 0$ . We assume that the turbulent Reynolds number is high enough for molecular diffusion to be negligible.

### A. Eddy-viscosity models

The problem is examined for the  $(k, \epsilon)$  turbulence model in its standard high-turbulent-Reynolds-number form. A similar analysis could be performed for any other two-equation model as long as turbulent diffusion is of the gradient type. Here, the set of governing equations is restricted to the turbulent-kinetic-energy ( $k$ ) and dissipation-rate ( $\epsilon$ ) equations in the simplified forms

$$0 = \frac{d}{dz} \left( \frac{\nu_t}{\sigma_k} \frac{dk}{dz} \right) - \epsilon, \tag{1a}$$

$$0 = \frac{d}{dz} \left( \frac{\nu_t}{\sigma_\epsilon} \frac{d\epsilon}{dz} \right) - C_{\epsilon 2} \frac{\epsilon^2}{k}, \tag{1b}$$

where  $\nu_t = C_\mu k^2 / \epsilon$  is the eddy viscosity;  $\sigma_k$ ,  $\sigma_\epsilon$ ,  $C_\mu$  and  $C_{\epsilon 2}$  are the usual modeling constants. One has to solve these equations with the following boundary conditions:

$$k(z=0) = k_0, \quad \epsilon(z=0) = \epsilon_0,$$

$$\lim_{z \rightarrow \infty} k(z) = 0, \quad \lim_{z \rightarrow \infty} \epsilon(z) = 0.$$

We shall look for similarity solutions considering that, at any  $z$ , the spatial evolution of the variables cannot depend on other quantities than the local levels of turbulent kinetic energy and dissipation rate. On dimensional grounds, this reads as

$$\frac{dk}{dz} = \alpha \frac{\epsilon}{k^{1/2}} \quad \text{and} \quad \frac{d\epsilon}{dz} = \beta \frac{\epsilon^2}{k^{3/2}}, \tag{2}$$

where  $\alpha$  and  $\beta$  are nondimensional constants to be determined by substituting relations (2) in Eqs. (1a) and (1b). It appears that the only solution that satisfies the boundary condition at infinity is obtained with

$$\alpha = -\sqrt{\frac{2\sigma_k}{3C_\mu}} \quad \text{and} \quad \beta = \sqrt{\frac{\sigma_k}{24C_\mu}} - \sqrt{\frac{\sigma_k}{24C_\mu} + \frac{C_{\epsilon 2}\sigma_\epsilon}{C_\mu}}.$$

Now, the derivative of the turbulent length scale  $l = k^{3/2} / \epsilon$  can be directly deduced from relations (2):

$$\frac{dl}{dz} = \frac{3}{2} \alpha - \beta. \tag{3}$$

Integration is immediate and gives

$$l = l_0 + \gamma z \quad \text{with} \quad l_0 = \frac{k_0^{3/2}}{\epsilon_0} \quad \text{and} \quad \gamma = \frac{3\alpha - 2\beta}{2}.$$

The dissipation rate can therefore be written as  $k^{3/2} / (l_0 + \gamma z)$  and relations (2) be integrated to

$$\frac{k}{k_0} = \left(1 + \gamma \frac{z}{l_0}\right)^{\alpha/\gamma} \quad \text{and} \quad \frac{\epsilon}{\epsilon_0} = \left(1 + \gamma \frac{z}{l_0}\right)^{\beta/\gamma}.$$

This fully determines the solution and shows that the only similarity solutions [in the sense of Eq. (2)] are power solutions with a linear variation of the length scale. Now, physical considerations as well as experimental evidence show that the length scale should increase with the distance from the source. According to Eq. (3), this requires that  $\gamma > 0$  and leads to the following condition on the modeling constants:

$$2\sigma_k - C_{\epsilon 2}\sigma_\epsilon < 0. \tag{4}$$

Introducing the combination of constants  $\Lambda = C_{\epsilon 2}\sigma_\epsilon/\sigma_k$ , the decrease exponents of the turbulent kinetic energy and dissipation rate can be rewritten as

$$\frac{\alpha}{\gamma} = \frac{-7 - \sqrt{1 + 24\Lambda}}{6(\Lambda - 2)} \quad \text{and} \quad \frac{\beta}{\gamma} = \frac{1 - 4\Lambda - \sqrt{1 + 24\Lambda}}{4(\Lambda - 2)}.$$

The slope of the length scale is given by

$$\gamma = \sqrt{\frac{\sigma_k}{24C_\mu}(\sqrt{1 + 24\Lambda} - 7)}$$

and condition (4) becomes:  $\Lambda > 2$ . We note that, if  $\Lambda$  takes the value 10/3, then  $\alpha/\gamma = -2$ , so that the rms value of the velocity fluctuation decreases as  $1/z$ , as indicated by the majority of experimental data. With the standard set of constants<sup>22</sup>

$$\sigma_k = 1, \quad \sigma_\epsilon = 1.3, \quad C_\mu = 0.09 \quad \text{and} \quad C_{\epsilon 2} = 1.92,$$

one gets  $\alpha = -2.72$ ,  $\beta = -4.63$ ,  $\gamma = 0.55$  and

$$\frac{k}{k_0} = \left(1 + 0.55 \frac{z}{l_0}\right)^{-4.95}, \quad \frac{\epsilon}{\epsilon_0} = \left(1 + 0.55 \frac{z}{l_0}\right)^{-8.42}.$$

Thus, the decrease of turbulent kinetic energy is significantly overestimated—Long’s theory and the majority of experimental data give  $k \propto z^{-2}$ —and consequently, the Reynolds-number evolution takes the form of a  $z^{-1.47}$  decrease. The latter result leaves the possibility for a low-turbulent-Reynolds-number regime at large  $z$ . Such a regime is not compatible with the concept of “grid action” (according to which, the turbulent Reynolds number should be constant throughout the flow) but is reminiscent of what is observed in the situation of decreasing homogeneous turbulence.<sup>23</sup>

These differences between model behavior and well-established experimental trends is evidently linked with the low value of  $\Lambda$  obtained with the standard constants: about 2.5 to be compared with our preferred value 10/3. This implies that either the value of  $C_{\epsilon 2}$  or that of the ratio  $\sigma_\epsilon/\sigma_k$  is too small. The value of  $C_{\epsilon 2}$  is usually chosen in the range 1.8 to 2 in order to match the rate of decay of homogeneous turbulence, so that things may be difficult to improve by simply adjusting this value. Instead, a number of arguments support the idea of increasing the ratio  $\sigma_\epsilon/\sigma_k$ . First, an analysis of direct-numerical-simulation data for wall-bounded flows by Cazalbou and Bradshaw<sup>24</sup> indicates that the standard value  $\sigma_\epsilon = 1.3$  is consistent with the data while a value of  $\sigma_k$  in the range 0.4 to 0.7 should be preferred in the outer layer. These authors also pointed out that such a low

value could be incompatible with the existence of a well-defined boundary layer edge. However, lowering  $\sigma_k$  to 0.75 while keeping  $C_{\epsilon 2}$  and  $\sigma_\epsilon$  to their standard values would bring  $\Lambda$  fairly close to 10/3 without violating the edge constraint ( $\sigma_\epsilon < 2\sigma_k$ , see Ref. 21). On another hand, recent attempts to reoptimize the  $(k, \epsilon)$  model by Davodet *et al.*<sup>25,26</sup> and in the framework of the AVTAC European Community project (see Bézard<sup>27</sup>) also lead to an increase in the ratio  $\sigma_\epsilon/\sigma_k$  (respectively, 1.3/0.8 and 1.14/0.58 for the references cited) with improvements in the prediction of a variety of flows including wall-bounded flows and free shear flows.

Some variants of the  $(k, \epsilon)$  model display an even lower value of  $\Lambda$  than the standard version and condition (4) can be violated.<sup>28,29</sup> In this case,  $\gamma$  is negative and powers of  $(1 + \gamma z/l_0)$  are undefined for  $z/l_0 > -1/\gamma$ . However, it could be shown that the evolution given by

- $k/k_0 = (1 + \gamma z/l_0)^{\alpha/\gamma}$  and  $\epsilon/\epsilon_0 = (1 + \gamma z/l_0)^{\beta/\gamma}$ , for  $0 \leq z < -1/\gamma$ , and
- $k$  and  $\epsilon$  are uniform for  $z \geq -1/\gamma$  and as small as wanted provided that  $\nu_t$  remains finite,

corresponds to a weak solution of the *steady* diffusion problem when  $\Lambda < 2$  (not to be confused with the weak solutions given by Cazalbou *et al.*<sup>21</sup> in the *propagation* regime). From a numerical point of view, we have checked that this solution was obtained at time convergence of the unsteady problem with the calculation method used in Sec. III. So, violation of condition (4) produces solutions for which turbulence *partially* contaminates the surrounding space: on a distance  $(l_0/\gamma)$  that does not exceed a few integral length scales (about three for the models cited above). Such a behavior, along with the decrease of the length scale with distance from the source, is difficult to accept on physical grounds but practical consequences of this deficiency have not been further explored here.

The limiting case  $\Lambda = 2$  corresponds to a constant length scale throughout the flow. The turbulent kinetic energy and dissipation rate experience an exponential spatial decay according to

$$k = k_0 \exp\left(\alpha \frac{z}{l_0}\right) \quad \text{and} \quad \epsilon = \epsilon_0 \exp\left(\beta \frac{z}{l_0}\right),$$

with

$$\alpha = \frac{2}{3}\beta = -\sqrt{\frac{2\sigma_k}{3C_\mu}}.$$

### B. Reynolds-stress transport models

At the second-order-closure level, the problem is governed by two equations for the normal Reynolds stresses  $\overline{u^2}$  and  $\overline{w^2}$  (axisymmetric state) supplemented with the dissipation-rate equation. Taking into account the simplifications of the problem, the exact transport equation of the Reynolds stress  $u_i u_j$  ( $u_i$  is the velocity fluctuation along  $x_i$  relative to the statistical average denoted by an overbar) can be written as

TABLE I. Turbulent-diffusion and return-to-isotropy models considered in the steady problem.

Turbulent diffusion		
Daly and Harlow (Ref. 30)	$-\overline{u_i u_j u_k} = C_s \frac{k}{\epsilon} \overline{u_i u_j} \frac{\partial u_k}{\partial x_l}$	$C_s = 0.22$
Hanjalic and Launder (Ref. 31)	$-\overline{u_i u_j u_k} = C_s \frac{k}{\epsilon} G_{ijk}$	$C_s = 0.11$
Mellor and Herring (Ref. 32)	$-\overline{u_i u_j u_k} = C_s (k^2/\epsilon) [(\overline{\partial u_i u_j / \partial x_k}) + (\overline{\partial u_i u_k / \partial x_j}) + (\overline{\partial u_j u_k / \partial x_i})]$	$C_s = 0.2$
Lumley (Ref. 19) ( $D_{ij}^u$ )	$-\overline{u_i u_j u_k} = C_{s1} (k/\epsilon) (G_{ijk} + C_{s2} (G_{iil} \delta_{jk} + G_{jll} \delta_{ik} + G_{kll} \delta_{ij}))$	$\begin{cases} C_{s1} = 0.185 \\ C_{s2} = 0.066 \end{cases}$
Lumley (Ref. 19) ( $D_{ij}^p$ )	$-\overline{p u_i'} / \rho = P_D \overline{u_i u_i'}$	$P_D = 1/5$
$\pi_{ij} / \epsilon$		
Rotta (Ref. 33)	$-C_1 a_{ij}$	$C_1 = 1.8$
Fu <i>et al.</i> (Ref. 34)	$-C_1 \mathbf{A}^{1/2} \mathbf{A}_2 (a_{ij} + C_1' (a_{ik} a_{kj} - \mathbf{A}_2 \delta_{ij}/3)) - a_{ij} (1 - \mathbf{A}^{1/2})$	$\begin{cases} C_1 = 7.5 \\ C_1' = 0.6 \end{cases}$
Sarkar and Speziale (Ref. 35)	$-C_1 a_{ij} + C_2 (a_{ik} a_{kj} - \mathbf{A}_2 \delta_{ij}/3)$	$\begin{cases} C_1 = 1.7 \\ C_2 = 1.05 \end{cases}$
$G_{ijk} = \overline{u_i u_j} \frac{\partial u_k}{\partial x_l} + \overline{u_j u_i} \frac{\partial u_k}{\partial x_l} + \overline{u_k u_i} \frac{\partial u_j}{\partial x_l}, \quad a_{ij} = \frac{\overline{u_i u_j}}{k} - \frac{2}{3} \delta_{ij}$ $\mathbf{A}_2 = a_{ij} a_{ji}, \quad \mathbf{A}_3 = a_{ij} a_{jk} a_{ki}, \quad \mathbf{A} = 1 - \frac{9}{8} (\mathbf{A}_2 - \mathbf{A}_3)$		

$$0 = \frac{\partial}{\partial x_k} \left( \underbrace{-\overline{u_i u_j u_k} - \frac{\overline{p u_i}}{\rho} \delta_{jk} - \frac{\overline{p u_j}}{\rho} \delta_{ik}}_{D_{ij}} \right) + \underbrace{\frac{p}{\rho} \left( \frac{\partial u_j}{\partial x_i} + \frac{\partial u_i}{\partial x_j} \right)}_{\Pi_{ij}} - 2 \underbrace{v \left( \frac{\partial u_i}{\partial x_k} \frac{\partial u_j}{\partial x_k} \right)}_{\epsilon_{ij}} \quad (5)$$

$D_{ij}$ ,  $\Pi_{ij}$  and  $\epsilon_{ij}$  are, respectively, the turbulent diffusion term (by pressure and velocity fluctuations), the pressure-strain term (reduced to its ‘‘slow’’ part due to the absence of mean-velocity gradients) and the dissipation term (with  $\epsilon = \epsilon_{ii}/2$ ). Lumley’s rearrangement can be used to form a unique return-to-isotropy term:  $\pi_{ij} = \Pi_{ij} - \epsilon_{ij} + 2/3 \epsilon \delta_{ij}$ , so that Eq. (5) finally becomes

$$0 = D_{ij} + \pi_{ij} - 2/3 \epsilon \delta_{ij},$$

leaving turbulent diffusion and return-to-isotropy as the only processes that need to be modeled. We shall consider the same closure schemes as Straatman *et al.*<sup>18</sup> Their definitions and references<sup>19,30–35</sup> are given in Table I. The return-to-isotropy schemes are linear (Rotta<sup>33</sup>), quadratic (Sarkar and Speziale<sup>35</sup>) and quadratic with a formulation that accounts for the anisotropy of the dissipation tensor (Fu, Launder and Tselepidakis<sup>34</sup>). All turbulent-diffusion schemes are of gradient type and neglect pressure diffusion with the exception of Lumley’s.<sup>19</sup> Concerning this scheme, we use the following relations between the diffusion constants and  $C_1$ , the return-to-isotropy constant in Rotta’s scheme (see Shih, Lumley and Janicka<sup>36</sup>):  $C_{s1} = 2/(3\beta)$  and  $C_{s2} = (\beta - 2)/(4\beta + 10)$  with  $\beta = 2C_1$ . The resulting values are significantly different from those used by Straatman *et al.* These authors have re-

produced what we believe is a misinterpretation by Schwarz and Bradshaw<sup>37</sup> of the relation between the diffusion and return-to-isotropy constants.

The dissipation-rate model equation can be taken in a standard form. In the absence of mean velocity, it reads as

$$0 = \frac{\partial}{\partial x_i} \left( C_\epsilon \overline{u_i u_j} \frac{\partial \epsilon}{\partial x_j} \right) - C_{\epsilon 2} \frac{\epsilon^2}{k},$$

with  $C_\epsilon = 0.14$  and  $C_{\epsilon 2} = 1.92$ .

The analysis performed for eddy-viscosity models can be adapted with little changes considering that

- $\overline{u^2} = \overline{v^2}$ , and
- the equation for  $\overline{u^2}$  can be replaced by that for the turbulent kinetic energy.

Accordingly, the problem is governed by the following system:

$$0 = D_k - \epsilon, \quad (6a)$$

$$0 = D_{33} + \pi_{33} - 2/3 \epsilon, \quad (6b)$$

$$0 = D_\epsilon - C_{\epsilon 2} \epsilon^2/k, \quad (6c)$$

where  $D_{33}$ ,  $D_k = D_{ii}/2$  and  $D_\epsilon$  denote, respectively, the turbulent-diffusion terms of  $w^2$ ,  $k$  and  $\epsilon$ . We shall look for a similarity solution satisfying

$$\frac{dk}{dz} = \alpha \frac{\epsilon}{k^{1/2}}, \quad \frac{d\epsilon}{dz} = \beta \frac{\epsilon^2}{k^{3/2}} \quad \text{and} \quad \frac{\overline{w^2}}{u^2} = a^2. \quad (7)$$

The equilibrium value of the anisotropy ratio  $a$  will be a result of the analysis. It follows that relations (7) cannot be valid for  $z=0$  if turbulence is produced with an anisotropy level that does not match the equilibrium value to be found.

TABLE II. Turbulent-diffusivity coefficients obtained with the different gradient schemes used.

	$f(a)$	$g(a)$	$h(a)$
Daly and Harlow (Ref. 30)	$C_s \frac{2a^2}{2+a^2}$	$C_s \frac{2a^2}{2+a^2}$	$C_\epsilon \frac{2a^2}{2+a^2}$
Hanjalic and Launder (Ref. 31)	$C_s \frac{2a^2(3a^2+2)}{(2+a^2)^2}$	$3C_s \frac{2a^2}{2+a^2}$	"
Mellor and Herring (Ref. 32)	$C_s \frac{3a^2+2}{2+a^2}$	$3C_s$	"
Lumley ( $D_{ij}$ ) (Ref. 19)	$C_{s1} \frac{2a^2(3a^2+2)(1+5C_{s2})}{(2+a^2)^2}$	$6C_{s1} \frac{a^2(1+3C_{s2})+2C_{s2}}{2+a^2}$	"
Lumley ( $D_{ij}^p$ ) (Ref. 19)	$-2P_D C_{s1} \frac{2a^2(3a^2+2)(1+5C_{s2})}{(2+a^2)^2}$	$-2P_D C_{s1} \frac{2(3a^2+2)(1+5C_{s2})}{2+a^2}$	

We shall therefore consider our results as applicable to a similarity region away from the source and we can assume—as usual in this kind of problem—that  $z$  denotes the distance to a virtual origin whose location depends on the models used and the anisotropy level of the actual source.

We can proceed in the analysis noting that, whatever the diffusion model is (see Table II), it is possible to write

$$D_k = \frac{d}{dz} \left( f(a) \frac{k^2}{\epsilon} \frac{dk}{dz} \right),$$

$$D_{33} = \frac{d}{dz} \left( g(a) \frac{k^2}{\epsilon} \frac{dw^2}{dz} \right),$$

$$D_\epsilon = \frac{d}{dz} \left( h(a) \frac{k^2}{\epsilon} \frac{d\epsilon}{dz} \right).$$

It follows that Eqs. (6a) and (6c) can be solved as in the case of an eddy-viscosity model with the following solution, which now depends on the value of  $a$ :

$$\frac{k}{k_0} = \left( 1 + \gamma \frac{z}{l_0} \right)^{\alpha/\gamma}, \quad \frac{\epsilon}{\epsilon_0} = \left( 1 + \gamma \frac{z}{l_0} \right)^{\beta/\gamma}, \quad (8a)$$

with

$$\alpha = -\sqrt{\frac{2}{3f(a)}}, \quad \beta = \sqrt{\frac{1}{24f(a)}} - \sqrt{\frac{1}{24f(a)} + \frac{C_{\epsilon 2}}{h(a)}}. \quad (8b)$$

$\gamma$  is still equal to  $3\alpha/2 - \beta$  and the analog of condition (4) is  $2h(a) - C_{\epsilon 2}f(a) < 0$ . Relations (8a) and (8b) can be then substituted in Eq. (6b) to give

$$0 = \frac{2a^2}{2+a^2} \times \frac{g(a)}{f(a)} + \frac{\pi_{33}}{\epsilon} - \frac{2}{3}. \quad (9)$$

In this flow configuration and for all the return-to-isotropy models used,  $\pi_{33}/\epsilon$  is a literal function of  $a$  only (see Table III) and the solution of Eq. (9) allows the equilibrium value of  $a$  to be determined. A numerical solution to Eq. (9) is easily obtained, relations (8a) and (8b) then allow to fully determine the state of the flow. The corresponding results are given in Table IV with

- the decrease of turbulence characterized by the exponent  $n = \alpha/(2\gamma)$  of the rms value ( $u'$ ) of the fluctuation, and
- the evolution of the length scale, by the slope  $\gamma_L = \gamma(u'^2/k)^{3/2}$ .

$\gamma_L$  can be assimilated to the slope of the integral scale relative to  $u$  along  $x$  ( $L_x^u$ ) since the relation  $L_x^u = \mathcal{A}u'^3/\epsilon$  seems to be satisfied with  $\mathcal{A}=1$  in our configuration (see Kit *et al.*<sup>6</sup>).

In spite of the approximations made in their analysis, the anisotropy levels reported by Straatman *et al.*<sup>18</sup> are in agreement with the values obtained here. This can be traced to the

TABLE III.  $\pi_{33}/\epsilon$  as a function of  $a$  for return-to-isotropy models.

Model	$\pi_{33}/\epsilon$
Rotta (Ref. 33)	$C_1 \left( \frac{2}{3} - \frac{2a^2}{2+a^2} \right)$
Fu <i>et al.</i> (Ref. 34)	$(C_1 \mathbf{A}^{1/2} \mathbf{A}_2 + 1 - \mathbf{A}^{1/2}) \left( \frac{2}{3} - \frac{2a^2}{2+a^2} \right) - \frac{1}{3} C_1 C_1' \mathbf{A}^{1/2} \mathbf{A}_2^2$
Sarkar and Speziale (Ref. 35)	$C_1 \left( \frac{2}{3} - \frac{2a^2}{2+a^2} \right) + \frac{1}{3} C_2 \mathbf{A}_2$

$$\mathbf{A}_2 = \frac{8}{3} \frac{(a^2-1)^2}{(2+a^2)^2}, \quad \mathbf{A}_3 = \frac{16}{9} \frac{(a^2-1)^3}{(2+a^2)^3}, \quad \mathbf{A} = \frac{a^2(8a^2+19)}{(2+a^2)^3}$$

TABLE IV. Similarity results obtained far from the source in the steady state with the different Reynolds-stress-transport models.

Return to isotropy	Diffusion	$n$	$\gamma_L$	$a$
Rotta (Ref. 33)	Daly and Harlow (Ref. 30)	-1.28	0.46	1
	Hanjalic and Launder (Ref. 31)	-1.00	0.19	1.75
	Mellor and Herring (Ref. 32)	-0.50	0.31	1.75
	Lumley (Ref. 19) ( $D_{ij}$ )	-0.32	0.47	1.60
	Lumley (Ref. 19) ( $D_{ij} + D_{ij}^p$ )	-0.97	0.56	1
Fu <i>et al.</i> (Ref. 34)	Daly and Harlow (Ref. 30)	-1.28	0.46	1
	Hanjalic and Launder (Ref. 31)	-1.14	0.22	1.55
	Mellor and Herring (Ref. 32)	-0.47	0.41	1.55
	Lumley (Ref. 19) ( $D_{ij}$ )	-0.33	0.52	1.52
	Lumley (Ref. 19) ( $D_{ij} + D_{ij}^p$ )	-0.97	0.56	1
Sarkar and Speziale (Ref. 35)	Daly and Harlow (Ref. 30)	-1.27	0.46	1
	Hanjalic and Launder (Ref. 31)	-0.60	0.01	6.88
	Mellor and Herring (Ref. 32)	-0.65	0.007	6.88
	Lumley (Ref. 19) ( $D_{ij}$ )	-0.29	0.28	2.08
	Lumley (Ref. 19) ( $D_{ij} + D_{ij}^p$ )	-0.97	0.56	1

fact that their hypothesis lead to the correct (linear) evolution of the length scale. A conclusion of both analysis is that no combination of models is able to produce an anisotropy level in the range 1.1 to 1.4 as indicated by the experimental and simulation data. This can be explained upon considering that in this flow, anisotropy is generated by turbulent diffusion and return to isotropy only comes to moderate this effect. As a matter of fact, Eq. (9) shows that when the diffusion coefficients for  $w^2$  and  $k$  are equal:  $f(a)=g(a)$  for all  $a$  with Daly and Harlow scheme or  $f(1)=g(1)$  when  $P_D=1/5$  with Lumley's scheme, no anisotropy is generated and  $a$  remains unity whatever the return-to-isotropy scheme is. Hanjalic-Launder and Mellor-Herring diffusion schemes exhibit the same ratio  $g(a)/f(a)$  and it can be easily seen that Lumley's scheme without pressure diffusion produces a lower ratio as soon as  $a$  is higher than unity. Thus, Hanjalic-Launder and Mellor-Herring diffusion schemes always give the same value of  $a$  when combined with the same return-to-isotropy scheme, while Lumley's scheme without pressure diffusion always returns a lower value. Now, with the linear scheme of Rotta as a reference for return to isotropy, we see that the nonlinear schemes do not react in the same way to an over-generation of anisotropy by the diffusion scheme. The Fu *et al.* scheme seems to compensate for this effect while the Sarkar-Speziale scheme amplifies it. The reason is that the latter has been devised to reduce the rate of return to isotropy for high values of  $A_3$  (corresponding to high values of  $A_2$  in our configuration), in agreement with experimental data. The high values of  $a$  (6.88) obtained in our configuration should therefore not question the accuracy of Sarkar-Speziale scheme. As a matter of fact, we shall see below that, when the diffusion scheme is adjusted so as to keep generation of anisotropy in reasonable bounds, the results obtained with this scheme are beyond criticism.

Our analysis gives also access to the decrease exponent of  $u'$  and to the slope of the length scale. Considering the former, we mentioned above that the body of experimental data indicates that  $n=-1$  but values of  $-0.86$  and  $-1.5$  have also been reported. Values higher than  $-1$  are difficult

to accept from a physical point of view since, together with the linear increase of the length scale, they would imply a turbulent Reynolds number increasing with  $z$ . So, if we consider  $-1.5$  to  $-1$  as a plausible range for  $n$ , every return-to-isotropy scheme considered here can be combined with several diffusion schemes to produce a decrease exponent in this range. Considering the slope  $\gamma_L$  of the length scale, experiments with oscillating grids give a rather wide scatter, it seems that this value depends strongly on the particular geometry of the grid, frequency and stroke (see Refs. 5 and 6). Measurements by Thompson and Turner<sup>4</sup> gave  $\gamma_L=0.1$ , Hopfinger and Toly<sup>5</sup> reported three values in the range 0.16 to 0.34 while Kit *et al.*<sup>6</sup> gave a value of 0.25. Such a sensitivity to the initial parameters of the turbulence source is indeed out of reach of one-point closure but, with one exception, the tested models produce values that stay in line with the data.

From a practical point of view, the analysis provides some guidelines to improve model performances in this flow configuration. Straatman *et al.*<sup>18</sup> emphasized that modeling pressure diffusion was necessary to accurately predict anisotropy and suggested to use Lumley's model with a lowered value of  $P_D$ . Our analysis indeed supports this conclusion but also suggests an optimization strategy; noting that the value of  $a$  does not depend on the constants in the dissipation equation [see Eq. (9)], one can proceed in two steps: (i) adjust the value of  $P_D$  in order to get the proper level of anisotropy; and (ii) adjust the diffusion constant  $C_\epsilon$  to obtain the correct spatial decrease. At this stage, we neither wish to modify the diffusion constants in the Reynolds-stress equations, since they are connected to the return-to-isotropy constant by construction—nor  $C_{\epsilon 2}$ —whose value is usually fixed by the decay law of homogeneous turbulence. Such an optimization performed with the target values  $a=1.2$  and  $n=-1$  gives  $P_D=0.17$  and  $C_\epsilon=0.175$  when Rotta's return-to-isotropy scheme is used, and  $P_D=0.18$  and  $C_\epsilon=0.17$  with the Sarkar-Speziale scheme. In both cases,  $\gamma_L$  takes the value 0.35 which is perfectly acceptable in view of the experimental data cited above. The optimized values of  $C_\epsilon$  are

consistent with usual implementations of Reynolds-stress-transport models. Note that we were unable to perform a similar optimization with the Fu *et al.* scheme: it seems that, in this case, the evolution of  $a$  when  $P_D$  varies in the range 0 to 1/5 is not continuous and that values of  $a$  in the range 1 to 1.4 cannot be reached.

In a recent paper, not available when this one was submitted, Straatman<sup>38</sup> proposed a calibration procedure based on the approximate analysis of Straatman *et al.*<sup>18</sup> and the simulation results of Briggs *et al.* The method allows to determine the values of  $C_{s2}$  and  $P_D$  in Lumley's model and ensures that the three terms at work in this model are balanced in agreement with the simulation data. This appears to be linked with the value of the ratio  $R_1 = \overline{u^2 w} / \overline{w^3}$  in a selected region of the flow. Taking  $R_1 = 0.29$ , Straatman obtained  $C_{s2} = 0.31$  and  $P_D = 0.153$  with the return-to-isotropy scheme of Sarkar and Speziale. These values are significantly different from those used or obtained here but do not really conflict with our analysis: following Straatman's method the value  $C_{s2} = 0.066$  can be recovered by taking  $R_1 \approx 0.25$  which leads to  $P_D \approx 0.18$  in agreement with the result of our optimization.  $R_1 \approx 0.25$  is not far from the value recommended by Straatman and equally supported by the simulation data. It remains that the large difference between possible values of  $C_{s2}$  is a matter of concern and a precise evaluation of this model constant should probably be done using a different approach.

### III. UNSTEADY PROBLEM

We turn now to the unsteady problem in which the source is switched on at  $t = 0$ . At a given time  $t$ , turbulence will have diffused over some distance and we shall look for a time-dependent scaling of the instantaneous profiles of the different variables. As we shall see below, the solution of the steady-state problem will provide a useful basis for such a scaling.

We restrict the analysis to the case of the  $(k, \epsilon)$  model and the unsteady problem is governed by the following set of equations:

$$\frac{\partial k}{\partial t} = \frac{\partial}{\partial z} \left( \frac{\nu_t}{\sigma_k} \frac{\partial k}{\partial z} \right) - \epsilon, \tag{10a}$$

$$\frac{\partial \epsilon}{\partial t} = \frac{\partial}{\partial z} \left( \frac{\nu_t}{\sigma_\epsilon} \frac{\partial \epsilon}{\partial z} \right) - C_{\epsilon 2} \frac{\epsilon^2}{k}, \tag{10b}$$

with the initial condition:

$$\forall z > 0 \quad k(z, t=0) = 0, \quad \epsilon(z, t=0) = 0,$$

and the boundary conditions:

$$\forall t \geq 0 \quad \begin{cases} k(z=0, t) = k_0, \\ \epsilon(z=0, t) = \epsilon_0, \\ \lim_{z \rightarrow \infty} k(z, t) = 0, \\ \lim_{z \rightarrow \infty} \epsilon(z, t) = 0. \end{cases}$$

It has been shown by Cazalbou *et al.*<sup>21</sup> that, if the ratio  $\sigma_\epsilon / \sigma_k$  is lower than 2, turbulence propagates into the undisturbed fluid at a finite velocity. At a given time, the evolutions of the different variables can be analytically described

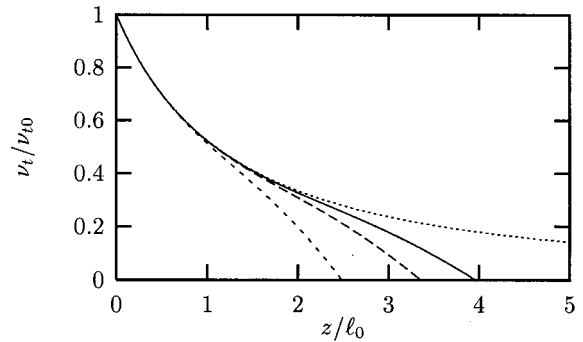


FIG. 1. Numerical solution of the unsteady  $(k, \epsilon)$  model problem, eddy-viscosity profiles. ---,  $t\epsilon_0/k_0 = 30$ ; —,  $t\epsilon_0/k_0 = 60$ ; —,  $t\epsilon_0/k_0 = 90$ ; ····,  $(1 + \gamma z/l_0)^{(2\alpha - \beta)/\gamma}$  (steady solution).

in the vicinity of the front and correspond to a weak solution of the model equations there. To better visualize the characteristics of such solutions, numerical integration of Eqs. (10a) and (10b) can be carried out using the method presented in the Appendix. The resulting eddy-viscosity profiles at three different times are plotted in Fig. 1 together with the steady solution. The propagation character of the solution is apparent: the eddy viscosity goes to zero linearly (a general characteristic of the weak solutions given in Ref. 21) at a finite distance from the source. As time proceeds, so does the position of the front  $\delta(t)$  and one is inclined to look for a similarity solution in the form  $k = K(t)f(\eta)$  and  $\epsilon = E(t)g(\eta)$  with  $\eta = z/\delta(t)$ . However,  $\delta$  is not the only time-dependent length scale to enter the problem and this method is not able to give a solution valid at all times. This is apparent in Fig. 2 where we plot the instantaneous profile of the length scale at a given time: in addition to  $\delta(t)$  a second time-dependent scale,  $l_\infty(\delta)$ , is to be considered (the suffix  $\infty$  will denote the value of the variable in the steady solution at the location given between parentheses, here: the position of the front  $\delta$ ). It is therefore difficult to imagine a simple way to scale the solution at  $t$  and, in order to proceed, we shall have to consider separately the cases of “short” and “long” times.

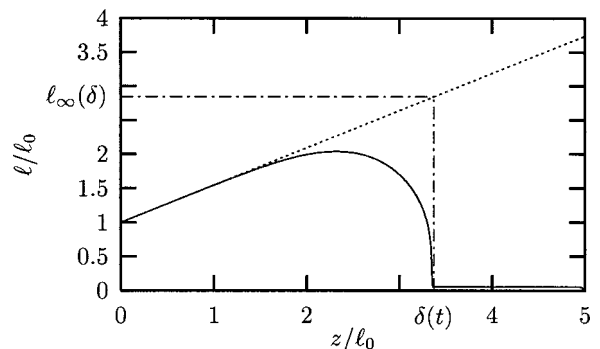


FIG. 2. Illustration of the different time-dependent length scales in the unsteady  $(k, \epsilon)$  model problem. —, Length-scale profile at  $t\epsilon_0/k_0 = 60$ ; ····,  $1 + \gamma z/l_0$  (steady solution).

**A. Short-time scaling**

We define short times by considering that, in the corresponding regime, (i) turbulence has diffused over a short distance (compared to the length scale at the source  $l_0$ ) and (ii) the value of the length scale in the steady solution at  $z = \delta$  remains close to  $l_0$ . We have therefore simultaneously

$$\delta \ll l_0 \quad \text{and} \quad l_\infty(\delta) \approx l_0 \quad \text{so that} \quad \delta \ll l_\infty(\delta).$$

As a direct consequence, gradients are important and diffusion dominates all. We get a pure-diffusion problem that can be described by the following system:

$$\frac{\partial k}{\partial t} = \frac{\partial}{\partial z} \left( \frac{\nu_t}{\sigma_k} \frac{\partial k}{\partial z} \right), \tag{11a}$$

$$\frac{\partial \epsilon}{\partial t} = \frac{\partial}{\partial z} \left( \frac{\nu_t}{\sigma_\epsilon} \frac{\partial \epsilon}{\partial z} \right), \tag{11b}$$

with the same initial and boundary conditions as the original diffusion/destruction problem.  $\delta(t)$  is the relevant characteristic length scale and we shall look for a similarity solution in the form

$$k = k_0 f(\eta) \quad \text{and} \quad \epsilon = \epsilon_0 g(\eta) \quad \text{with} \quad \eta = \frac{z}{\delta(t)}, \tag{12}$$

where  $\delta$  is more generally considered as *proportional* to the position of the front. Substituting these expressions in Eqs. (11a) and (11b), we get

$$-\frac{\sigma_k}{C_\mu} \frac{\epsilon_0}{k_0^2} \delta \dot{\delta} \eta f' = \left( \frac{f^2 f'}{g} \right)',$$

$$-\frac{\sigma_\epsilon}{C_\mu} \frac{\epsilon_0}{k_0^2} \delta \dot{\delta} \eta g' = \left( \frac{f^2 g'}{g} \right)',$$

where  $(\cdot)$  and  $(\cdot)'$  denote, respectively, time and  $\eta$  derivatives. Solutions in the form of Eq. (12) exist only if

$$\frac{\epsilon_0}{C_\mu k_0^2} \delta \dot{\delta} = A,$$

$A$  being a nondimensional constant.  $A$  is arbitrary and simply sets the *constant* ratio between the position of the front and  $\delta(t)$ . Integration of the last equation yields the expressions of the position of the front and propagation velocity  $c(t) = \dot{\delta}$ , that is

$$\delta(t) = \sqrt{\frac{2AC_\mu k_0^2}{\epsilon_0}} \times \sqrt{t} \quad \text{and} \quad c(t) = \sqrt{\frac{AC_\mu k_0^2}{2\epsilon_0}} \times \frac{1}{\sqrt{t}}. \tag{13}$$

The self-similar profiles are then the solutions of the system

$$-A \sigma_k \eta f' = \left( \frac{f^2 f'}{g} \right)', \tag{14a}$$

$$-A \sigma_\epsilon \eta g' = \left( \frac{f^2 g'}{g} \right)', \tag{14b}$$

with

$$f(0) = g(0) = 1 \quad \text{and} \quad \lim_{\eta \rightarrow \infty} f(\eta) = \lim_{\eta \rightarrow \infty} g(\eta) = 0.$$

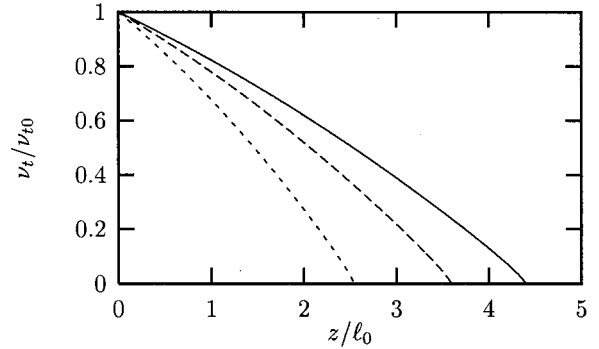


FIG. 3. Numerical solution of the pure-diffusion unsteady  $(k, \epsilon)$  model problem, eddy-viscosity profiles. ---,  $t\epsilon_0/k_0=30$ ; - · -,  $t\epsilon_0/k_0=60$ ; —,  $t\epsilon_0/k_0=90$ .

There is no straightforward analytical solution to Eq. (14a)–(14b), but Eqs. (11a)–(11b) can be numerically integrated. The result of such an integration is illustrated in Figs. 3 and 4. The contamination, at a finite velocity, of the flow is apparent in Fig. 3 where the eddy-viscosity profiles are plotted for three distinct values of time. In Fig. 4, the same data are replotted according to the theoretical self-similar scaling [ $z$  normalized by  $(tk_0^2/\epsilon_0)^{1/2}$ ]. The three profiles collapse on a single curve that can be considered as the solution of (14a)–(14b) with  $A=1/(2C_\mu)$ . This confirms the validity of the time evolutions given by Eq. (13). One can notice that in the one-equation model of Spalart and Allmaras,<sup>20</sup> the absence of a destruction term in the eddy-viscosity equation enables the distinction between short and long times to be eliminated and the  $t^{-1/2}$  behavior of the propagation velocity could be shown to be valid all along the evolution. Such a behavior is remarkably consistent with the results of Long’s analysis and known experimental data.

**B. Long-time scaling**

In the long-time regime we consider that

$$\delta(t) \gg l_0 \quad \text{and therefore} \quad \delta(t) \approx l_\infty(\delta).$$

Since  $k$  and  $\epsilon$  are both decreasing with  $z$  in the steady state, we can also assume that, for  $t$  sufficiently large, we have

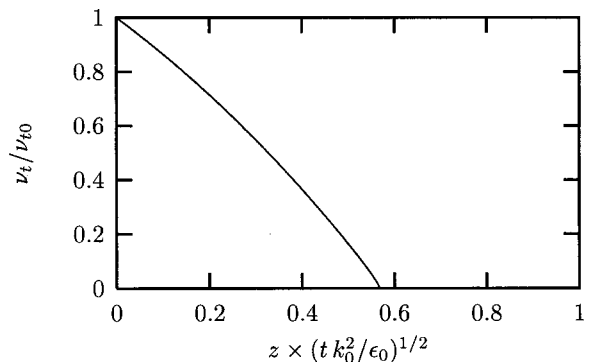


FIG. 4. Numerical solution of the pure-diffusion unsteady  $(k, \epsilon)$  model problem. Eddy-viscosity profiles as functions of  $z$  scaled by the theoretical expression of  $\delta(t)$  (13). ---,  $t\epsilon_0/k_0=30$ ; - · -,  $t\epsilon_0/k_0=60$ ; —,  $t\epsilon_0/k_0=90$ ; the three profiles, perfectly collapsing, are indistinguishable.

$$k_0 \gg k_\infty(\delta) \quad \text{and} \quad \epsilon_0 \gg \epsilon_\infty(\delta).$$

This precludes any scaling based on the values of the variables at the source and it seems that  $\delta(t)$  can only be considered as a reference location at  $t$ . Thus, we look for a solution in the form

$$\begin{aligned} k &= K(t)f(\eta) & \text{with} & \quad \eta = \frac{\delta(t) - z}{K^{3/2}(t)/E(t)}. \\ \epsilon &= E(t)g(\eta) \end{aligned} \quad (15)$$

As previously, relations (15) can be substituted in Eqs. (10a)–(10b) to give

$$\frac{C_\mu}{\sigma_k} \left( \frac{f^2 f'}{g} \right)' = \left[ \frac{\dot{\delta}}{K^{1/2}} \right] f' - \left[ \frac{3}{2} \frac{\dot{K}}{E} - \frac{K\dot{E}}{E^2} \right] \eta f' + \left[ \frac{\dot{K}}{E} \right] f + g, \quad (16a)$$

$$\begin{aligned} \frac{C_\mu}{\sigma_\epsilon} \left( \frac{f^2 g'}{g} \right)' &= \left[ \frac{\dot{\delta}}{K^{1/2}} \right] g' - \left[ \frac{3}{2} \frac{\dot{K}}{E} - \frac{K\dot{E}}{E^2} \right] \eta g' + \left[ \frac{K\dot{E}}{E^2} \right] g \\ &+ C_{\epsilon 2} \frac{g^2}{f}. \end{aligned} \quad (16b)$$

Here again, a necessary condition for the system to have a self-similar solution is that the terms between brackets are constant, which is equivalent to

$$\frac{\dot{\delta}}{K^{1/2}} = A, \quad \frac{\dot{K}}{E} = B, \quad \frac{K\dot{E}}{E^2} = C, \quad (17)$$

where  $A$ ,  $B$  and  $C$  are nondimensional constants. Now, it is easy to check that this condition can be fulfilled if one takes for  $K$  and  $E$  the solution for  $k$  and  $\epsilon$  in the steady state at  $z = \delta(t)$ :

$$K(t) = k_0 \left( 1 + \gamma \frac{\delta(t)}{l_0} \right)^{\alpha/\gamma}, \quad (18a)$$

$$E(t) = \epsilon_0 \left( 1 + \gamma \frac{\delta(t)}{l_0} \right)^{\beta/\gamma}. \quad (18b)$$

Accordingly, relations (17) are satisfied with  $B = A\alpha$ ,  $C = A\beta$  and the following expression for  $\delta(t)$ :

$$\frac{\delta(t)}{l_0} = \frac{1}{\gamma} \left( A_0 t \frac{\epsilon_0}{k_0} + A_1 \right)^{\gamma/(\alpha-\beta)} - \frac{1}{\gamma}, \quad (19)$$

where  $A_0 = A(\alpha - \beta)$  and  $A_1$  is an integration constant. Incidentally, we note that the value of the exponent only depends on the choice of the modeling constants through the value of  $\Lambda$ :

$$\frac{\gamma}{\alpha - \beta} = \frac{12(\Lambda - 2)}{12\Lambda - 17 + \sqrt{1 + 24\Lambda}}.$$

Differentiation of Eq. (19) gives the expression of the propagation velocity:

$$c(t) = A k_0^{1/2} \left[ A_0 t \frac{\epsilon_0}{k_0} + A_1 \right]^{\alpha/2(\alpha-\beta)} = A \sqrt{k_\infty(\delta)}. \quad (20)$$

Provided that relations (17) are satisfied, the remaining spatial problem is governed by the following equations:

$$\frac{C_\mu}{A\sigma_k} \left( \frac{f^2 f'}{g} \right)' - \frac{g}{A} - f'(1 - \gamma\eta) - \alpha f = 0,$$

$$\frac{C_\mu}{A\sigma_\epsilon} \left( \frac{f^2 g'}{g} \right)' - C_{\epsilon 2} \frac{g^2}{A f} - g'(1 - \gamma\eta) - \beta g = 0.$$

If we consider that the value of  $A$  has been chosen so that  $\delta(t)$  corresponds *strictly* to the position of the front at  $t$ , relations (15) show that  $f$  and  $g$  need to be defined on the interval  $[0, 1/\gamma]$  which is the limit when  $\delta$  goes to infinity of  $[0, \delta/(l_0 + \gamma\delta)]$  (corresponding to  $z$  in  $[\delta, 0]$ ). The boundary conditions at  $\eta = 0$  are immediate, we have:  $f(0) = 0$  and  $g(0) = 0$ . To specify the boundary conditions at  $\eta = 1/\gamma$ , we begin by writing relations (15) for  $z = 0$ :

$$1 = \left( 1 + \gamma \frac{\delta}{l_0} \right)^{\alpha/\gamma} f \left( \frac{\delta}{l_0 + \gamma\delta} \right),$$

$$1 = \left( 1 + \gamma \frac{\delta}{l_0} \right)^{\beta/\gamma} g \left( \frac{\delta}{l_0 + \gamma\delta} \right),$$

$\delta$  varying from 0 to infinity. Introducing  $X = \delta/(l_0 + \gamma\delta)$ , we get  $\delta/l_0 = X/(1 - \gamma X)$  and it follows that, for all  $X$  between 0 and infinity,  $f(X) = (1 - \gamma X)^{\alpha/\gamma}$  and  $g(X) = (1 - \gamma X)^{\beta/\gamma}$ . Obviously this result is not acceptable for  $X = 0$ , so that in the end, the analysis appears to be restricted to the case where  $X$  remains close to  $1/\gamma$  that is  $\delta \gg l_0$  which is characteristic of the long-time regime. We shall therefore consider the following boundary condition at  $\eta = 1/\gamma$ :

$$f(\eta) \underset{\eta \rightarrow 1/\gamma}{\sim} (1 - \gamma\eta)^{\alpha/\gamma} \quad \text{and} \quad g(\eta) \underset{\eta \rightarrow 1/\gamma}{\sim} (1 - \gamma\eta)^{\beta/\gamma}. \quad (21)$$

The analysis is now complete. It shows that, in the unsteady model problem, a similarity solution in the form of Eq. (15) with time-dependent characteristic scales given by Eqs. (18a)–(18b) is adequate at large times. With the standard set of constants, the position of the front should evolve as  $t^{0.29}$ . A remarkable result is that, when  $\Lambda$  takes the value 10/3 (corresponding to a  $1/z$  decrease in the steady problem), the position of the front evolves as  $t^{1/2}$  in the long-time regime as required by Long's theory.

Numerical integration of Eqs. (10a)–(10b) has been carried out to check these results. According to Eq. (19), the quantity  $\Delta = (\delta/l_0 + 1/\gamma)^{(\alpha-\beta)/\gamma}$  should be a linear function of time during the propagation. It is rather easy to locate the position of the front in the numerical solution and to plot it against time. This has been done in Fig. 5, the linear character of the result at large times is quite convincing while a slow divergence at short times is apparent. A least-square linear approximation of the curve in the range  $t = 5$  to 90 gives  $A_0 = 0.9$  and  $A_1 = 2.1$  corresponding to  $A = 0.47$ . The propagation velocity has been plotted in Fig. 6 together with the time evolution of  $k_\infty(\delta)$ . Both curves are in good agreement as soon as  $t = 5$ , the slope of the logarithmic plot being consistent with the exponent in Eq. (20). As  $t$  becomes lower than 5, the two curves depart significantly and  $c(t)$  exhibits the  $-1/2$  slope, characteristic of the pure-diffusion regime at short times.

If we turn now to the space problem, it can be seen in Fig. 7 that the eddy-viscosity profiles, computed at three dif-

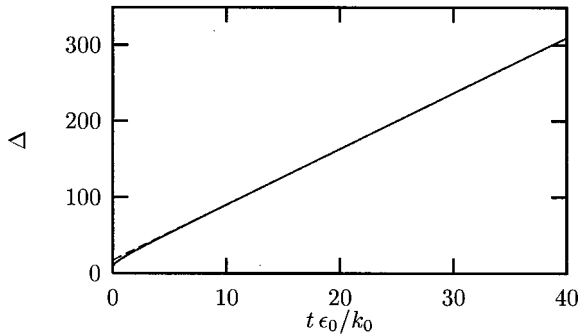


FIG. 5. Time evolution of  $\Delta = (\delta/l_0 + 1/\gamma)^{(\alpha-\beta)/\gamma}$ . —, Numerical result; ---, least-square linear fit between  $t=5$  and  $t=90$ .

ferent times in the long-time regime, perfectly collapse when scaled according to Eqs. (15), (18a) and (18b). One also observes that the equivalent of relation (21) for the eddy viscosity

$$f^2(\eta)/g(\eta) \underset{\eta \rightarrow 1/\gamma}{\sim} (1 - \gamma\eta)^{(2\alpha-\beta)/\gamma}$$

accurately fits the results as soon as  $\eta=0.4$ . According to the analysis in Cazalbou *et al.*,<sup>21</sup> the slope of the eddy-viscosity profile at the front should be equal to  $A(2\sigma_k - \sigma_\epsilon)/C_\mu$ , the corresponding line is plotted on the figure with  $A=0.47$  and is in good agreement with the numerical result.

**C. Transition between short and long times**

As time progresses from  $t=0$ , the space evolution gradually shifts from the short-time situation where the turbulence flux at the source ( $\phi_{k0} = (\nu_t/\sigma_k) \partial k/\partial z|_{z=0}$ ) decreases in modulus (it should reach zero in the end if the evolution were to proceed in the pure-diffusion regime) to the long-time situation where it saturates on the constant value corresponding to the steady state, that is:

$$\lim_{t \rightarrow \infty} \phi_{k0} = \frac{C_\mu}{\sigma_k} \frac{k_0^2}{\epsilon_0} \frac{\partial k_\infty}{\partial z} \Big|_{z=0} = \alpha \frac{C_\mu}{\sigma_k} k_0^3,$$

and, similarly for the dissipation rate:

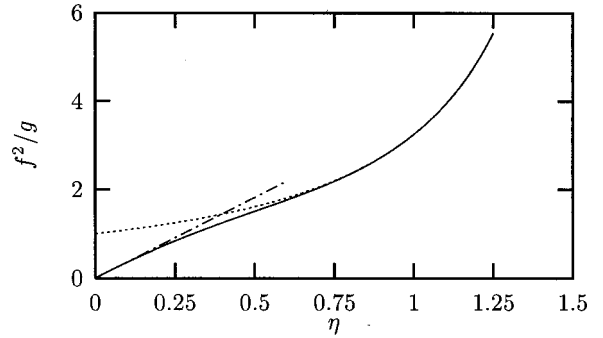


FIG. 7. Eddy-viscosity profiles in the long-time regime scaled by the time-dependent characteristic scales. ---,  $t\epsilon_0/k_0=30$ ; —,  $t\epsilon_0/k_0=60$ ; ···,  $t\epsilon_0/k_0=90$ ; ····, asymptotic behavior when  $\eta \rightarrow 1/\gamma$ ; -·-·-, theoretical slope of the eddy-viscosity profile at the front [ $A(2\sigma_k - \sigma_\epsilon)$  with  $A=0.47$ ]. The three instantaneous profiles, collapsing perfectly, are indistinguishable.

$$\lim_{t \rightarrow \infty} \phi_{\epsilon 0} = \frac{C_\mu}{\sigma_\epsilon} \frac{k_0^2}{\epsilon_0} \frac{\partial \epsilon_\infty}{\partial z} \Big|_{z=0} = \beta \frac{C_\mu}{\sigma_\epsilon} k_0^{1/2} \epsilon_0.$$

Figure 8 shows the time behavior of these fluxes and one sees that, starting from theoretically infinite values at  $t=0$ , they come to saturation on the above values for a nondimensional time approximately equal to 3. Rigorously this is only obtained when  $t \rightarrow \infty$ . However, one can give an indication of the time ( $t_T$ ) at which transition between the short- and long-time regimes occurs by noting in Fig. 4 that the gradient of  $\nu_t$  at the source takes the constant value 1.28 when  $z$  is scaled by  $(tk_0^2/\epsilon_0)^{1/2}$ . Equating with the known value in the steady solution we get

$$t_T \epsilon_0/k_0 = (1.28/(\beta - 2\alpha))^2 \approx 2.47,$$

which is coherent with what can be observed in Fig. 8. Moreover, noticing in Fig. 4 that the front is located at  $z \approx 0.57k_0^{3/2}/\epsilon_0$ , it can be deduced that  $t_T$  correspond to a propagation distance of the same order of magnitude as the integral scale at the source:  $\delta_T \approx 0.9k_0^{3/2}/\epsilon_0$ . This is a rather short distance and, consequently, it is most likely that the experimental data for the propagation of the front should be compared with model solutions in the long-time regime.

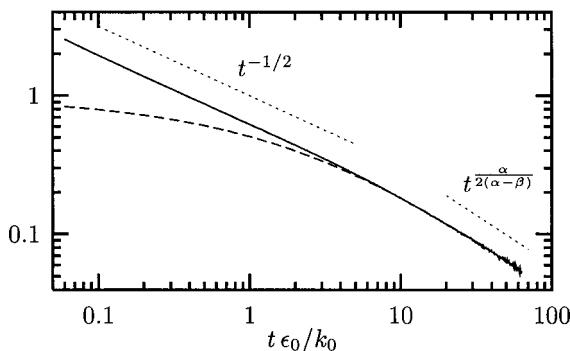


FIG. 6. Time evolution of the propagation velocity. —, Numerical result for  $c(t)/A$  with  $A=0.47$ ; ---,  $k_\infty(\delta)$ ,  $\delta(t)$  being given by the numerical solution.

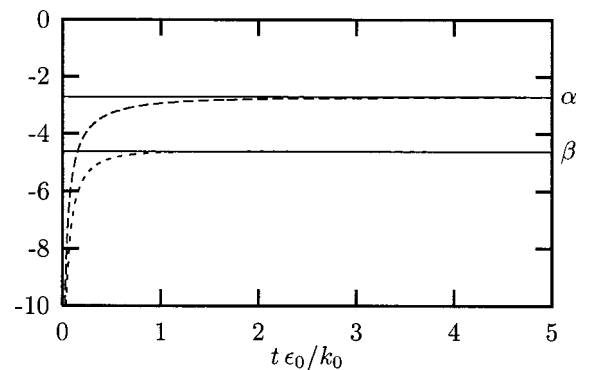


FIG. 8. Time evolutions of the turbulent-kinetic-energy and dissipation-rate fluxes at  $z=0$ . —,  $\phi_{k0} \times \sigma_k / (C_\mu k_0^3)$ ; ---,  $\phi_{\epsilon 0} \times \sigma_\epsilon / (C_\mu k_0^{1/2} \epsilon_0)$ .

#### IV. SUMMARY AND CONCLUSION

It has been shown that a number of characteristics of the turbulent field created by the diffusion from a plane source could be analytically given for turbulence models of first and second order. In the steady state, complete solutions where turbulence usually fills the whole surrounding space can be obtained: the spatial decrease of turbulence, as well as the equilibrium anisotropy level for a variety of second-order models are given and may be used to improve the performances of the models in this flow configuration.

With the two-equation eddy-viscosity models that satisfy the conditions given in Ref. 21, one can also examine the problem at finite times. It appears that the cases of short and long times have to be distinguished. The first case corresponds to a pure-diffusion evolution, the position of the front evolves as  $t^{1/2}$  whatever the values of the model constants are. The evolution at large times is slowed down by viscous dissipation and the position of the front still evolves as a decreasing power of time but the exponent now depends on the model constants. With the standard  $(k, \epsilon)$  model, transition between short- and long-time regimes occurs after a period of time which is of the order of the integral scale at the source.

If some constraints on the modeling constants are taken into account, the agreement with experimental data is always satisfactory from a qualitative point of view. For the prediction of the steady state with the  $(k, \epsilon)$  model, the combination of constants  $\Lambda = C_{\epsilon 2} \sigma_k / \sigma_\epsilon$  should be higher than 2 for allowing (i) the length scale to increase when the turbulent kinetic energy decreases and (ii) turbulence to fill the whole surrounding space. An equivalent constraint holds for second-order models. In the propagation regime, the constraint  $\sigma_\epsilon / \sigma_k < 2$  given in Ref. 21 is still desirable. Finally, a remarkable value for  $\Lambda$  (10/3) ensures a hyperbolic spatial decrease of the rms value of the velocity fluctuation in the steady regime and a parabolic time behavior for the progression of the front in the propagation regime at large times, in agreement with existing experimental data. It seems that re-considering the calibration of the  $(k, \epsilon)$  model so as to respect this particular value of  $\Lambda$  could be done without major difficulty.

#### ACKNOWLEDGMENTS

Remarks from the referees helped to precise the implications of the analysis and to strengthen the conclusions of the paper. The authors gratefully acknowledge them here.

#### APPENDIX: NUMERICAL DETAILS

In Sec. III, we use a rather classical numerical method to solve the closure equations. It is based on a time-marching procedure with finite-volume discretizations in space and time.

The time discretization is first-order accurate, implicit for diffusion and explicit for destruction. The time step must be very small at  $t=0$  where the propagation velocity tends to infinity and can be relaxed as time proceeds: we make it vary as  $\sqrt{t}$  from  $5 \times 10^{-4}$  at  $t=0$  up to  $1.25 \times 10^{-2}$  at  $t=60$  (all

values normalized by  $k_0/\epsilon_0$ ). About 9000 time steps are therefore needed to compute the flow during this period of time.

The space discretization is conservative with a constant step, 600 grid points are used up to  $z/l_0=5$ .

The turbulent kinetic energy and its dissipation rate cannot be set to zero in the undisturbed fluid. As in Ref. 21, we use "small" but non-zero values there:  $10^{-3}$  times their respective level at the source.

The instantaneous position of the front is determined with an accuracy of one mesh size which is enough to examine its behavior. After differentiation, however, it returns a propagation velocity that can be rather noisy. The results for this quantity (Fig. 6) are evaluated every 80 time steps from a linear least-square fit of the front position for these 80 steps. Time resolution remains very good, the corresponding time intervals being in the range  $6 \times 10^{-2}$  at the beginning of the calculation to 1 at the end.

- <sup>1</sup>S. Corrsin and A. L. Kistler, "Free-stream boundaries of turbulent flows," NACA Report 1244, 1955.
- <sup>2</sup>R. R. Long, "Theory of turbulence in a homogeneous fluid induced by an oscillating grid," Phys. Fluids **21**, 1887 (1978).
- <sup>3</sup>S. C. Dickinson and R. R. Long, "Laboratory study of the growth of a turbulent layer of fluid," Phys. Fluids **21**, 1698 (1978).
- <sup>4</sup>S. M. Thompson and J. S. Turner, "Mixing across an interface due to turbulence generated by an oscillating grid," J. Fluid Mech. **67**, 349 (1975).
- <sup>5</sup>E. J. Hopfinger and J.-A. Toly, "Spatially decaying turbulence and its relation to the mixing across density interfaces," J. Fluid Mech. **78**, 155 (1976).
- <sup>6</sup>E. L. G. Kit, E. J. Strang, and H. J. S. Fernando, "Measurements of turbulence near shear-free density interface," J. Fluid Mech. **334**, 293 (1997).
- <sup>7</sup>D. A. Briggs, J. H. Ferziger, J. R. Kosef, and S. G. Monismith, "Entrainment in a shear-free turbulent mixing layer," J. Fluid Mech. **310**, 215 (1996).
- <sup>8</sup>I. A. Hannoun, H. J. S. Fernando, and E. J. List, "Turbulence structure near a sharp density interface," J. Fluid Mech. **189**, 189 (1988).
- <sup>9</sup>I. P. D. De Silva and H. J. S. Fernando, "Some aspects of mixing in a stratified turbulent patch," J. Fluid Mech. **240**, 601 (1992).
- <sup>10</sup>I. P. D. De Silva and H. J. S. Fernando, "Oscillating grids as a source of nearly isotropic turbulence," Phys. Fluids **6**, 2455 (1994).
- <sup>11</sup>R. I. Nokes, "On the entrainment across a density interface," J. Fluid Mech. **188**, 185 (1988).
- <sup>12</sup>S. C. Dickinson and R. R. Long, "Oscillating-grid turbulence including effects of rotation," J. Fluid Mech. **126**, 315 (1983).
- <sup>13</sup>H. J. S. Fernando, "The growth of a turbulent patch in a stratified fluid," J. Fluid Mech. **190**, 55 (1988).
- <sup>14</sup>W. P. Jones and B. E. Launder, "The prediction of laminarization with a two-equation model of turbulence," Int. J. Heat Mass Transf. **15**, 301 (1972).
- <sup>15</sup>A. A. Sonin, "Calibration of the  $k-\epsilon$  model for the diffusion of turbulence," Phys. Fluids **26**, 2769 (1983).
- <sup>16</sup>G. L. Mellor and T. Yamada, "Development of a turbulence closure model for geophysical fluid problems," Rev. Geophys. Space Phys. **20**, 851 (1986).
- <sup>17</sup>D. C. Wilcox, "Reassessment of the scale determining equation for advanced turbulence models," AIAA J. **26**, 1299 (1988).
- <sup>18</sup>A. G. Straatman, G. D. Stubble, and G. D. Raithby, "Examination of diffusion modeling using zero-mean-shear turbulence," AIAA J. **36**, 929 (1998).
- <sup>19</sup>J. L. Lumley, "Computational modeling of turbulent flows," Adv. Appl. Mech. **18**, 123 (1978).
- <sup>20</sup>P. R. Spalart and S. R. Allmaras, "A one-equation turbulence model for aerodynamic flows," AIAA Paper No. 92-0439.
- <sup>21</sup>J.-B. Cazalbou, P. R. Spalart, and P. Bradshaw, "On the behavior of two-equation models at the edge of a turbulent region," Phys. Fluids **6**, 1797 (1994).

- <sup>22</sup>B. E. Launder and B. I. Sharma, "Application of the energy-dissipation model of turbulence to the calculation of flow near a spinning disk," *Lett. Heat Mass Transfer* **1**, 131 (1974).
- <sup>23</sup>G. K. Batchelor and A. A. Townsend, "Decay of isotropic turbulence in the final period," *Proc. R. Soc. London, Ser. A* **194**, 527 (1948).
- <sup>24</sup>J.-B. Cazalbou and P. Bradshaw, "Turbulent transport in wall-bounded flows. Evaluation of model coefficients using direct numerical simulation," *Phys. Fluids A* **5**, 3233 (1993).
- <sup>25</sup>O. Davodet, J.-C. Courty, J.-P. Bonnet, and S. Barre, "Augmentation de l'évasement de couches turbulentes cisailées libres compressibles: Calcul Navier-Stokes 3D  $k-\epsilon$ ," *Proc. 35ème Colloque d'Aérodynamique Appliquée, Analyse et contrôle des écoulements turbulents* (1999).
- <sup>26</sup>We refer to the set of constants named OD-JC in Ref. 25. Values of the turbulent Prandtl numbers were not given in the paper, those quoted here have been communicated by J.-C. Courty (private communication, 1999).
- <sup>27</sup>H. Bézard, "Optimisation of two-equation turbulence models," in *Advances in Turbulence VIII, Proceedings of the 8th European Conference*, 27–30 June 2000, Barcelona, Spain.
- <sup>28</sup>Y. Nagano, M. Tagawa, and T. Tsuji, "Effects of adverse pressure gradients on mean flows and turbulence statistics in a boundary layer," *Proceedings of the 8th Symp. on Turbulent Shear Flows, Munich* (1991).
- <sup>29</sup>V. Yakhot and S. A. Orszag, "Renormalization group analysis of turbulence theory. I. Basic theory," *J. Sci. Comput.* **1**, 3 (1986).
- <sup>30</sup>B. J. Daly and F. H. Harlow, "Transport equations in turbulence," *Phys. Fluids* **13**, 2634 (1970).
- <sup>31</sup>K. Hanjalić and B. E. Launder, "A Reynolds stress model of turbulence and its application to thin shear flows," *J. Fluid Mech.* **52**, 609 (1972).
- <sup>32</sup>G. L. Mellor and H. J. Herring, "A survey of mean turbulent field closure model," *AIAA J.* **11**, 590 (1973).
- <sup>33</sup>J. Rotta, "Statistische theorie nichthomogener turbulenz  $i$ ," *Z. Phys.* **129**, 547 (1951).
- <sup>34</sup>S. Fu, B. E. Launder, and D. P. Tselepidakis, "Accommodating the effects of high strain rates in modeling the pressure-strain correlation," UMIST, Dept. of Mechanical Engineering TFD/87/5, 1987.
- <sup>35</sup>S. Sarkar and C. G. Speziale, "A simple nonlinear model for the return to isotropy in turbulence," *Phys. Fluids A* **2**, 84 (1990).
- <sup>36</sup>T.-H. Shih, J. L. Lumley, and J. Janicka, "Second-order modeling of a variable-density mixing layer," *J. Fluid Mech.* **180**, 93 (1987).
- <sup>37</sup>W. R. Schwarz and P. Bradshaw, "Term-by-term tests of stress-transport turbulence models in a three-dimensional boundary layer," *Phys. Fluids* **6**, 986 (1994).
- <sup>38</sup>A. G. Straatman, "A modified model for diffusion in second-moment turbulence closures," *Trans. of the ASME, J. Fluid Eng.* **121**, 747 (1999).